J. Chem. Eng. Data **1984**, 29, 1-3

Thermal Conductivity of Molten Salts, HTS and the $LiNO_3$–$NaNO_3$ System, Using a Modified Transient Hot-Wire Method

T. Omotani and A. Nagashima*

Mechanical Engineering Department, Keio University, Hiyoshi, Yokohama 223, Japan

The thermal conductivity of salt mixtures, HTS and the $LiNO_3$–$NaNO_3$ system, was determined by using the modified transient hot-wire method. A newly developed apparatus with a mercury-in-glass probe was used at temperatures up to 593 K. The results for HTS (KNO_3–$NaNO_3$–$NaNO_2$, 44–7–49 mol %) showed very small temperature dependence in contrast to the large negative dependence given in some previous studies. The experimental data are given for the $LiNO_3$–$NaNO_3$ eutectic mixture for the first time.

Introduction

As high-temperature heat carriers, molten salts are important for energy technology. Among them, so-called HTS (or HTS 1, a mixture of 44 mol % KNO_3, 7 mol % $NaNO_3$, and 49 mol % $NaNO_2$) is used as a heat carrier as well as a thermal energy storage material. Lithium nitrate and its eutectic mixture with potassium have comparatively large fusion latent heat and thus are thought to be excellent heat storage materials. Although accurate knowledge of the thermal conductivity of these substances is essential for their application, the present state of our knowledge is far from satisfactory. As regards HTS, there exist considerable discrepancies among the available data, and, on the $LiNO_3$–$NaNO_3$ eutectic mixture, there are no experimental data available.

The present paper reports on measurements of the thermal conductivity of HTS, $LiNO_3$, and the $LiNO_3$–$NaNO_3$ eutectic mixture with the aid of a newly developed apparatus based on the transient hot-wire method at temperatures up to 593 K.

Experimental Procedure

The most important feature of the transient hot-wire method is that it can eliminate the error due to convection in the fluid layer, as explained in references concerning this conventional method (*1*). In order to apply this method to high-temperature melts which are electrically conducting, we developed a "liquid-metal" probe. The probe consists of a thin quartz mercury-filled capillary. Details of the principle and the calibration method were explained in our previous publications (*2*, *3*). The apparatus is shown in Figure 1. One leg of a quartz U-tube (1 in Figure 1) has a thin capillary portion. The whole U-tube is filled with mercury. The mercury was introduced into the capillary by applying a pressure of about 0.15 MPa at one end. Both ends of the U-tube have an inner diameter of 2.5 mm and the nickel terminals (1 mm in diameter) are immersed in mercury. The uppermost ends of the U-tube are covered with Teflon tops through which the nickel terminals penetrate leading to an outer electrical circuit. The dimensions of the probe were about 100 mm in effective length and 45 and 90 μm as regards its inner and outer diameters, respectively. Sample liquid 10 in container 2 was thermostated in salt bath 7. At time $t = 0$, the initial input of electrical current I was supplied to the probe. For small values of $a^2/(4kT)$, where a is the radius of the heater and k the thermal diffusivity of the sample fluid, the thermal conductivity equation is derived as

$$\lambda = (q/4\pi)/(\mathrm{d}\Delta V/\mathrm{d}\ln t) \qquad (1)$$

where q is the heat generated at the unit length of the heater, ΔT the temperature rise, and t the time.

In the present study, the temperature rise of the heater was replaced by an unbalanced voltage ΔV in a double bridge circuit. Thus, the working equation for the calculation of the thermal conductivity is

$$\lambda = \frac{1}{4\pi l_e} \frac{\mathrm{d}R}{\mathrm{d}T} \frac{RS}{R+S} I^3 \Big/ \left(\frac{\mathrm{d}\Delta V}{\mathrm{d}\ln t}\right) \qquad (2)$$

where R and S are resistances in the electrical circuit. Instrument constant l_e, the effective length of the test section, was calibrated against the thermal conductivity of toluene by Nagasaka and Nagashima (*1*). The temperature dependence of the resistivity of the mercury, $\mathrm{d}R/\mathrm{d}T$, was determined from the resistance measured over the whole temperature range. The term $\mathrm{d}\Delta V/\mathrm{d}\ln t$ was read from the recording of ΔV against time t on an X-Y recorder.

For our first apparatus (*2*) the probe was made of Pyrex glass. But later it was found that the electrical resistivity of Pyrex glass was insufficient at temperatures above 520 K (*3*). The material of the probe (capillary) was changed to quartz glass, which had much higher electrical resistivity at higher temperatures. In order to confirm the reliability of the present instrument, five probes were tested and results by different probes fell within the error limit. The data given in the present report are averages of 5–10 independent measurements under the same measuring conditions. Reproducibility was better than 1.8% at high temperatures.

A major part of the experimental error came from the uncertainties in the instrument constant l_e, the temperature coefficient of the electrical resistivity of mercury $\mathrm{d}R/\mathrm{d}T$, and the change in the unbalanced voltage against logarithmic time $\mathrm{d}\Delta V/\mathrm{d}\ln t$. The accuracy of the reference thermal conductivity of toluene was 0.5% (*1*); therefore, the uncertainty in instrument constant l_e was estimated to be 1.5%, considering reproducibility of calibration measurements with the present instrument. The error in the temperature coefficient of the resistivity of mercury $\mathrm{d}R/\mathrm{d}T$ was about 0.8% while the error in $\mathrm{d}\Delta V/\mathrm{d}\ln t$ was 0.3%. The mixing ratio of the sample was determined by weighing component salts with a chemical balance. The error in the mole fraction will not exceed 0.1%. Thus, considering also other minor error sources, the maximum uncertainty of the measured thermal conductivity was estimated at about 3%.

Results of HTS

In our first paper regarding this method (*2*), an example of measurement was given for HTS. But later, as mentioned in the previous section, deterioration of the resistivity of the Pyrex glass was observed at temperatures above 520 K. So the thermal conductivity of HTS was redetermined with a new probe made of quartz. The results are given in Table I. The most important thing about the new results is that the temperature dependence of the thermal conductivity is almost zero or very small. Although the data in Table I seem to show a small

0021-9568/84/1729-0001$01.50/0 © 1984 American Chemical Society

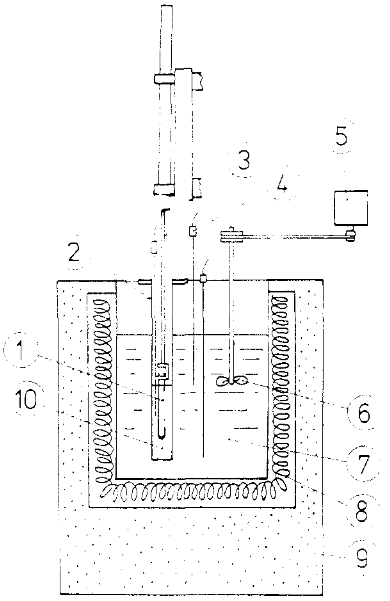

Figure 1. Apparatus for the measurement of the thermal conductivity: (1) capillary probe, (2) container, (3) rod, (4) resistance thermometer, (5) motor, (6) agitator, (7) salt bath, (8) electrical heater, (9) insulating material, (10) specimen.

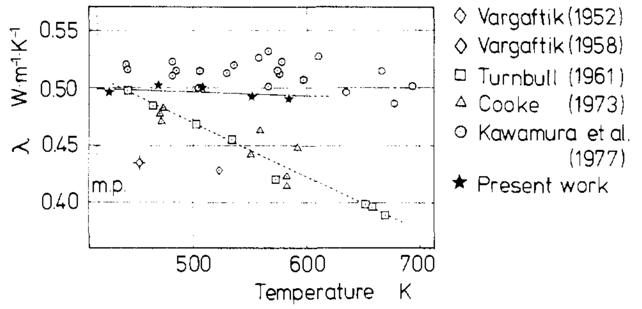

Figure 2. Thermal conductivity of HTS.

Table I. Measured Thermal Conductivity (λ) of HTS

temp, K	λ, W/(m·K)	SD[a]	temp, K	λ, W/(m·K)	SD[a]
426.7	0.497	0.001_3	509.0	0.502	0.002_8
427.4	0.491	0.002_8	552.8	0.494	0.001_6
469.4	0.504	0.003_2	583.8	0.492	0.005_5

[a] Standard deviation.

maximum at 469.4 K, we do not consider it meaningful since the difference between the highest and the lowest values is well within the experimental error. The fact that our old values were closely parallel to those of Turnbull (*4*), who used a bare metallic wire without any insulation in his transient hot-wire apparatus, suggests the considerable effect of electrical conductivity.

Our present data, as seen in Figure 2, show no or very small temperature dependence and agree reasonably well with the values reported by Odawara, Okada, and Kawamura (*5*), who used an optical method in the transient condition. In the case of other earlier studies (*6*–*8*) by the steady-state method, deviations from the previous results reach 10–20% at 593 K.

Results of the $LiNO_3$-$NaNO_3$ System

The thermal conductivity of $LiNO_3$ is given in Table II. As shown in Figure 3, the present data and those by Gustafsson (*9*) (also an optical method) show almost no dependence on temperature, although the latter are higher by 7–10%. Other data (*10*, *11*) lie in between and their agreement with the present results is better than that for HTS.

Table II. Measured Thermal Conductivity (λ) of the $LiNO_3$-$NaNO_3$

[$LiNO_3$], mol %	temp, K	λ, W/(m·K)	SD[a]
100	531.1	0.592	0.001_1
	549.0	0.590	0.004_3
	567.8	0.599	0.006_5
50	503.5	0.544	
	534.9	0.548	0.001_7
	566.0	0.545	0.003_8

[a] Standard deviation.

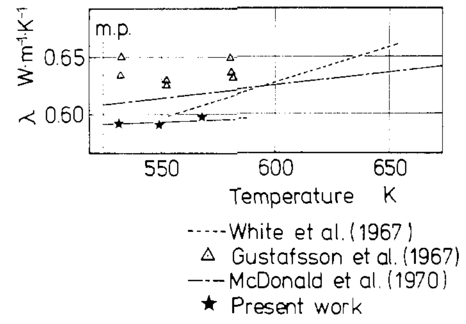

Figure 3. Thermal conductivity of $LiNO_3$.

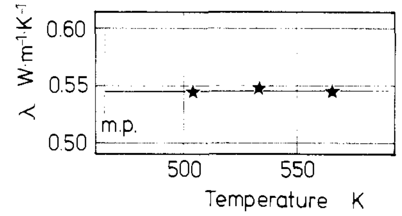

Figure 4. Thermal conductivity of $LiNO_3$-$NaNO_3$ mixtures (50-50 mol %).

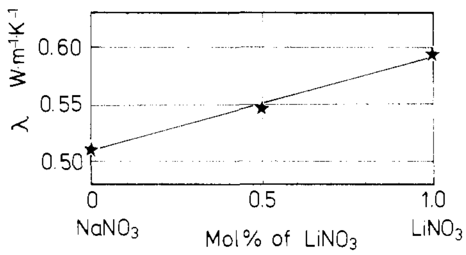

Figure 5. Thermal conductivity of $LiNO_3$-$NaNO_3$ system.

The eutectic mixture (50 mol %) of the $LiNO_3$-$NaNO_3$ system was also measured. The results are given in Table II and plotted in Figure 4. No previous studies were found for this mixture. In Figure 5 the data at 593 K are shown with values of $LiNO_3$ and $NaNO_3$, the latter also obtained by us (*3*). A linear dependence on composition is assumed for this mixture system considering the behavior of other salt systems such as the $NaNO_3$-KNO_3 system (*3*).

Conclusion

The thermal conductivity of molten salt mixtures, HTS and the eutectic $LiNO_3$-$NaNO_3$, and a single salt, $LiNO_3$, were measured in the temperature range from their melting points to 593 K by a modified transient hot-wire method using a liquid-metal in-capillary probe developed by us. Within the present temperature range no temperature dependence was detected for these mixtures and the single salt. The present results on HTS confirmed the necessity of electrical insulation of the heating element and suggested the insufficiency of the correction proposed in an earlier study. The composition dependence of the thermal conductivity of the $LiNO_3$–$NaNO_3$ system was also studied.

Glossary

a	radius of the heating element (outer diameter of the capillary), m
I	current, A
k	thermal diffusivity, m^2/s
l_e	instrument constant
q	heat generated at the unit length of the heater, W/m
R	electrical resistance, Ω
S	electrical resistance, Ω
t	time, s
T	temperature, K
ΔV	unbalanced voltage, V
λ	thermal conductivity, W/(m·K)

Registry No. $LiNO_3$, 7790-69-4; $NaNO_3$, 7631-99-4; KNO_3, 7757-79-1; $NaNO_2$, 7632-00-0.

Literature Cited

(1) Nagasaka, Y.; Nagashima, A. *Ind. Eng. Chem. Fundam.* **1981**, *20*, 216.
(2) Hoshi, M.; Omotani, T.; Nagashima, A. *Rev. Sci. Instrum.* **1981**, *52*, 755.
(3) Omotani, T.; Nagasaka, Y.; Nagashima, A. *Int. J. Thermophys.* **1982**, *3*, 17.
(4) Turnbull, A. G. *Aust. J. Appl. Sci.* **1961**, *12*, 30.
(5) Odawara, O.; Okada, I.; Kawamura, K. *J. Chem. Eng. Data* **1977**, *22*, 222.
(6) Vargaftik, N. V. *Izv. VTI* **1952**, *21*, 1.
(7) National Engineering Lab, "Liquid Thermal Conductivity—A Data Survey to 1973"; Her Majesty's Stationary Office: Scotland, 1975.
(8) Cooke, J. W. Report ORNL-4831; Oak Ridge National Laboratory: Oak Ridge, TN, 1973.
(9) Gustafsson, S. E.; Halling, N. O.; Kjellander, R. A. E. *Z. Naturforsh. A* **1968**, *23*, 682.
(10) Mcdonald, J.; Davis, H. T. *J. Phys. Chem.* **1970**, *74*, 725.
(11) White, L. R.; Davis, H. T. *J. Chem. Phys.* **1967**, *47*, 5433.

Received for review January 4, 1982. Revised manuscript received May 20, 1983. Accepted June 17, 1983.

Redox Electromotive Force Measurements in the Molten CuCl–CuCl$_2$ System and Thermodynamic Properties of Liquid CuCl$_2$. 1

Zafirios Glazitzoglou

Lehrstuhl für Technische Thermodynamik an der RWTH Aachen, 5100 Aachen, Federal Republic of Germany

Cu(I)/Cu(II) redox electromotive force measurements in the molten binary system CuCl–$CuCl_2$ were carried out by using a chlorine/chloride reference electrode in a temperature range from about 400 to 530 °C and for several concentrations up to 10 mol % $CuCl_2$. The free energy, enthalpy, and entropy change of the reaction $CuCl(l) + {}^1/_2Cl_2(g) = CuCl_2(l)$, as well as the unknown thermodynamic properties of molten solute $CuCl_2$, have been calculated as a function of temperature.

Introduction

No thermodynamic properties of pure molten $CuCl_2$ are included in the known collected thermodynamic data, such as in ref *1–4*. The reason is that $CuCl_2$ cannot exist in the pure fused state because of its decomposition already at the solid phase (*5*, *6*). Even the melting point values of $CuCl_2$ given in the literature differ widely between 498 and 633 °C (*4*, *6–8*).

The calculation of excess thermodynamic properties, as well as of activity coefficients, in a molten mixture requires the definition of a reference standard state for each liquid component. The purpose of the present work is to obtain experimentally the data necessary for the thermodynamic description of liquid cupric chloride. These investigations are part of an extensive study in order to determine the thermodynamic properties of the quaternary molten system CuCl–$CuCl_2$–KCl–LiCl by means of emf measurements.

The present study is the first in which redox potentials in the molten CuCl–$CuCl_2$ system were measured. Because of the volatility of the melt and the $CuCl_2$ decomposition, measurements have been made only up to 10 mol % $CuCl_2$. The heat capacity, the Gibbs energy, the entropy, the enthalpy, and the formation potential of molten solute $CuCl_2$ as well as the enthalpy and entropy of fusion were calculated from the data obtained.

The results can be used to estimate the thermodynamic quantities of several chemical processes in which copper chloride melts act as a reactant or catalyst. Among such thermodynamic calculations are, for example, reaction conversions for the chlorination of methane or other hydrocarbons (*7*, *9*), potentials for the electrolysis of molten cuprous chloride (*10*), equilibrium chlorine pressures, and the heat requirement for the chlorine production from cupric chloride (*7–9*).

Further, a knowledge of the Cu(I)/Cu(II) redox potentials in molten copper chloride mixtures is of significant importance in the understanding of the structure of these melts (*8*).

Experimental Section

The following electrochemical cell was used:

$$\ominus\, C \,\big|\, CuCl-CuCl_2(l) \,\vdots\, KCl-LiCl(l) \,\big|\, Cl_2(g),\, C\, \oplus$$

A diagram of this quartz cell is shown in Figure 1. A graphite rod surrounded by a quartz glass tube served as an indicator redox electrode. The chlorine–chloride reference electrode used (*11*) consists of a graphite tube immersed in molten KCl-LiCl eutectic (41.5 mol % KCl). Chlorine was bubbled through the melt. An asbestos diaphragm with a resistance of about 8000 Ω separates the two electrode compartments. The melt was contained in a quartz glass crucible. The temperature was measured with a calibrated NiCr–Ni thermocouple surrounded by a sheath of quartz glass. Cuprous chloride (Merck Darmstadt, FRG, No. 2739 p.a. minimum 98%) was dried under vacuum (10^{-3} mmHg) at 100 °C for 24 h to remove the main part of the moisture and then at 150 °C for a further 24 h. The eutectic (KCl Merck 4936 p.a. minimum 99.5%, LiCl Merck 5679 p.a. minimum 99%) was prepared according to the procedure described in ref *12* by melting under anhydrous HCl. Cupric chloride (Ventron Karlsruhe, FRG, No. 88759, anhydrous) was used directly. Chlorine (Linde Höllriegelskreuth, FRG,

0021-9568/84/1729-0003$01.50/0